

ISOCHRONS AND AL CONTAMINATION IN PRESOLAR GRAINS. E. Groopman¹, S. Amari¹, F. Gyngard¹, M. Jadhav², Y. Lin³, Y. Xu³, and E. Zinner¹, ¹Laboratory for Space Sciences, Washington University in St. Louis, MO 63130, USA, ²Dept. of the Geophysical Sciences, University of Chicago, IL 60637, USA, ³Institute of Geology and Geophysics, Chinese Academy of Sciences, Chaoyang, Beijing, CHN. (eegroopm@physics.wustl.edu)

Introduction: Presolar grains retain radiogenic daughter isotopes of radioactive ^{26}Al , ^{41}Ca , and ^{44}Ti , (e.g., [1]), among others, incorporated during the grains' formation. The initial presence of these radioactive isotopes is often indicative of a supernova (SN) origin. Zinner and Jadhav [1] constructed isochron-like correlation plots for the Al-Mg, Ca-K, and Ti-Ca systems from depth profiles of presolar graphite grains from Orgueil. Many of these isochrons show near-perfect correlations among $\delta^{26}\text{Mg}/^{24}\text{Mg}$ and $^{27}\text{Al}/^{24}\text{Mg}$, $\delta^{41}\text{K}/^{39}\text{K}$ and $^{40}\text{Ca}/^{39}\text{K}$, and $\delta^{44}\text{Ca}/^{40}\text{Ca}$ and $^{48}\text{Ti}/^{40}\text{Ca}$, indicating the retention of radiogenic ^{26}Mg , ^{41}K , and ^{44}Ca from the decays of ^{26}Al , ^{41}Ca , and ^{44}Ti , respectively. As [1] states, these are not true isochrons as they do not contain any temporal information; however, they resemble true isochrons and will be referred to as such in this abstract.

This study increases the number of isochrons extracted from presolar grain depth profiles to 67 and includes isochrons from both presolar graphite and SiC grains. The Al-Mg system is focused upon here for its simplicity regarding contamination, as there is only one stable Al isotope; however, the same kind of analysis may be applied to the other isotopic systems, such as Ca-K and Ti-Ca.

Methods: Isochrons reported in this abstract were derived from depth profiles of samples reported in previous studies, including presolar graphite grains from Orgueil [1–4], graphite grains from Murchison [5], and SiC from Murchison [6–7]. The grains' isotopic compositions indicate a likely SN origin.

Isochrons were generated by dividing NanoSIMS depth profiles into 5-cycle bins, where each point represents the average composition in a bin (Figures 1–2). Error bars indicate the standard error of the mean composition in each bin (Figure 2). Each isochron was fitted using Orthogonal Distance Regression (ODR; [8]), a least-squares regression technique that includes both x- and y-error weighting. The isochrons display the correlation between $\delta^{26}\text{Mg}/^{24}\text{Mg}$ and $^{27}\text{Al}/^{24}\text{Mg}$, whose slopes are related to the initial $^{26}\text{Al}/^{27}\text{Al}$ ratios by a factor of 1.393×10^{-4} (see [1]), assuming the $(^{26}\text{Mg}_{\text{intrinsic}}/^{24}\text{Mg})_{\text{sample}} \sim (^{26}\text{Mg}/^{24}\text{Mg})_{\text{standard}}$.

Results: The majority of grains analyzed in this study containing correlated $\delta^{26}\text{Mg}/^{24}\text{Mg}$ and $^{27}\text{Al}/^{24}\text{Mg}$ have isochrons that negatively intercepted the $\delta^{26}\text{Mg}/^{24}\text{Mg}$ axis, most often with values less than minus 1000 ‰ (Figure 2). As these values would other-

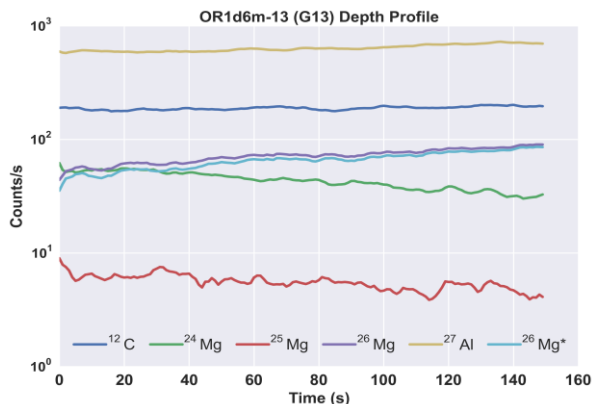


Figure 1: Depth profile of presolar graphite grain OR1d6m-13 (G13). Radiogenic ^{26}Mg ($^{26}\text{Mg}^*$) dominates the intrinsic ^{26}Mg signal. Profiles are smoothed for visual clarity.

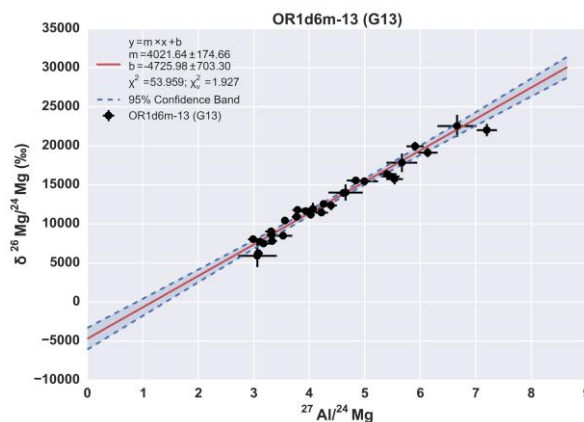


Figure 2: Al-Mg isochron from low-density presolar graphite grain G13. Errors on fit parameters are 1σ . The isochron slope of 4022 ± 175 corresponds to a $^{26}\text{Al}/^{27}\text{Al}$ ratio of $5.6 \times 10^{-1} \pm 2.4 \times 10^{-2}$. The $\delta^{26}\text{Mg}/^{24}\text{Mg}$ intercept of -4726 indicates that 27% of the measured Al is contamination.

wise correspond to negative intrinsic $^{26}\text{Mg}/^{24}\text{Mg}$ ratios, which are nonsensical, instead they indicate that these measurements were affected by constant Al contamination (see Appendix of [1]), which shifted the isochrons rightward and their $\delta^{26}\text{Mg}/^{24}\text{Mg}$ intercepts to more negative values. The data points for each isochron typically do not deviate drastically from the isochron fit, implying that the Al contamination did not change with sputtering depth. While models of core-collapse Type-II SNe (e.g., [9]) exhibit positive $\delta^{26}\text{Mg}/^{24}\text{Mg}$ values in their He/C and He/N zones, we may estimate a lower bound on the quantity of Al contamination in each measurement by solving for the horizontal shift required for the isochron to intercept the origin (Figure 3). The amount of Al contamination inferred from the

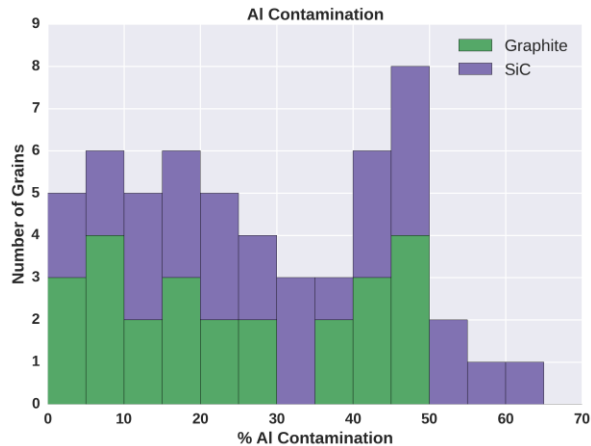


Figure 3: Estimated Al contamination (%) from isochrons with negative $\delta^{26}\text{Mg}/^{24}\text{Mg}$ intercepts. Histograms are stacked.

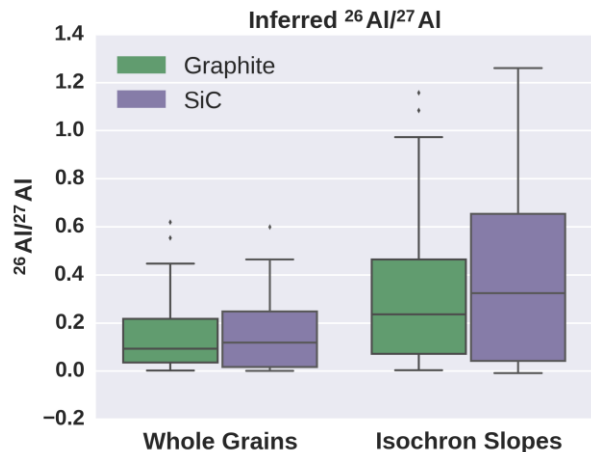


Figure 4: Differences in inferred initial $^{26}\text{Al}/^{27}\text{Al}$ ratios from isochron slopes and from whole-grain measurements. Whole-grain measurements underestimate the initial $^{26}\text{Al}/^{27}\text{Al}$ composition by more than a factor of two relative to the isochron slopes for both presolar SiC and graphite grains from SNe. Filled regions of the box plots show the interquartile range (IQR; 25 – 75%), with a median line; whiskers extend to $1.5 \times \text{IQR}$ past the closest quartile.

isochrons ranges up to 65% of the total $^{27}\text{Al}^+$ signal in some grain measurements, though the majority exhibit less than 50% Al contamination. Fifty-three of the 67 analyzed grains show that a significant fraction of their Al signal is not intrinsic. The distribution of Al contamination among the grains is not obviously peaked at any value and does not appear to be correlated with grain size. For the grains with isochrons intercepting the origin or the positive $\delta^{26}\text{Mg}/^{24}\text{Mg}$ axis, no Al contamination estimate could be made.

The distributions of initial $^{26}\text{Al}/^{27}\text{Al}$ composition are similar for presolar graphite and SiC SN grains for values derived from isochron slopes or from whole-grain measurements (Figure 4). The inferred initial $^{26}\text{Al}/^{27}\text{Al}$ ratios derived from isochron slopes differ from whole-grain measurements by a factor of 2.37 ± 0.11 (Figure 5). Linear regressions of the graphite and

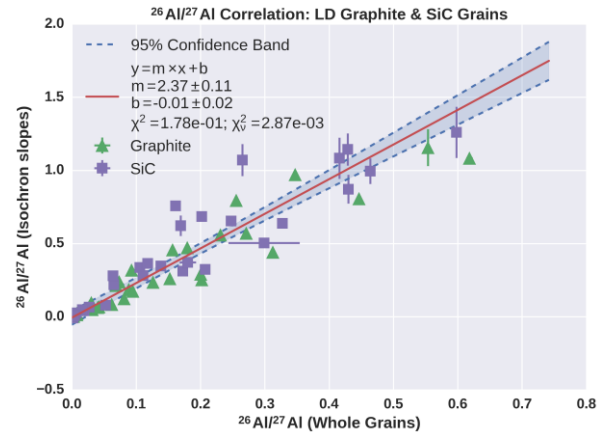


Figure 5: The inferred initial $^{26}\text{Al}/^{27}\text{Al}$ ratios from isochron slopes are ~ 2.4 times higher than those estimated from whole grain measurements. Linear regressions to only presolar graphite or SiC grains yielded slopes of 2.13 ± 0.13 and 2.52 ± 0.17 , respectively.

SiC grains separately yield slopes of 2.13 ± 0.13 and 2.52 ± 0.17 , respectively. For the majority of grains analyzed here, Al contamination appears to shift their isochrons rightward and their $\delta^{26}\text{Mg}/^{24}\text{Mg}$ intercepts to negative values, resulting in an underestimation of their intrinsic $^{26}\text{Al}/^{27}\text{Al}$ ratios.

Conclusions: The majority of grains analyzed exhibit significant contamination in their measured Al signals, often making it impossible to infer the initial $^{26}\text{Mg}/^{24}\text{Mg}$ ratio of the sample. For presolar grains whose isochrons positively intercept the $\delta^{26}\text{Mg}/^{24}\text{Mg}$ axis, whole-grain $^{26}\text{Al}/^{27}\text{Al}$ ratio calculations overestimate the true initial composition. The majority of isochrons, however, have negative $\delta^{26}\text{Mg}/^{24}\text{Mg}$ intercepts, often less than -1000‰ , implying the presence of significant Al contamination and leading to an underestimation of the true initial $^{26}\text{Al}/^{27}\text{Al}$ ratio in the whole-grain estimates. The quantity of uniform Al contamination may be estimated as the uniform shift required for the isochron to intercept the origin. The conventional whole-grain method for inferring initial $^{26}\text{Al}/^{27}\text{Al}$ ratios, by essentially forcing a linear fit through the origin, underestimates the isochron-derived $^{26}\text{Al}/^{27}\text{Al}$ ratios by a factor of ~ 2.5 .

References: [1] Zinner, E. and Jadhav, M. (2013) *ApJ*, 768, 100–118 [2] Jadhav, M. al. (2006) *New Astron. Rev.*, 50, 591–595 [3] Groopman, E. et al. (2012) *ApJL*, 754, L8–L13 [4] Jadhav, M. et al. (2013) *GCA*, 113, 193–224 [5] Amari, S. et al. (2014) *GCA* 133, 479–522 [6] Lin, Y. et al. (2010) *ApJ*, 709, 1157–1173 [7] Y. Xu et al. *ApJ*, in press. [8] Boggs, P. T. and Rogers, J. E. (1990) "Orthogonal Distance Regression" in *Contemporary Mathematics: Statistical Analysis of Measurement Error Models and Applications* (eds. P. J. Brown and W. A. Fuller) vol. 112 [9] Rauscher, T. et al. (2002) *ApJ*, 576, 323–348